Published in final edited form as:
J Bone Miner Res. 2013 July ; 28(7): 1531–1536. doi:10.1002/jbmr.1892.

A mouse model for human osteogenesis imperfecta type VI

Rosalind Bogan[1], **Ryan C. Riddle**[1,2], **Zhu Li**[1], **Sarvesh Kumar**[1], **Anjali Nandal**[1], **Marie-Claude Faugere**[3], **Adele Boskey**[4], **Susan E. Crawford**[5], and **Thomas L. Clemens**[1,2,*]

[1]Department of Orthopaedic Surgery, Johns Hopkins University School of Medicine, Baltimore, Maryland, USA

[2]Baltimore Veterans Administration Medical Center, Baltimore, Maryland, USA

[3]Department of Medicine, University of Kentucky, Lexington, Kentucky, USA

[4]Hospital for Special Surgery, New York, USA

[5]Department of Pathology, St. Louis University, St. Louis, Missouri, USA

Abstract

Osteogenesis imperfecta Type VI has recently be linked to a mutation in the *SERPINF1* gene which encodes Pigment Epithelium-Derived Factor (PEDF), a ubiquitously expressed protein originally described for its neurotrophic and anti-angiogenic properties. In this study, we characterized the skeletal phenotype of a mouse with targeted disruption of *Pedf*. In normal mouse bone, Pedf was localized to osteoblasts and osteocytes. MicroCT and quantitative bone histomorphometry in femurs of mature Pedf null mutants revealed reduced trabecular bone volume and the accumulation of unmineralized bone matrix. Fourier transform infrared microscopy (FTIR) indicated an increased mineral:matrix ratio in mutant bones which were more brittle than controls. *In vitro*, osteoblasts from Pedf null mice exhibited enhanced mineral deposition as assessed by alizarin red staining and an increased mineral:matrix determined by FTIR analysis of calcified nodules. The findings in this mouse model mimic the principal structural and biochemical features of bone observed in humans with OI type VI and consequently provide a useful model with which to further investigate the role of PEDF in this bone disorder.

Keywords

PEDF; osteogenesis imperfecta; bone mineralization

Introduction

Osteogenesis imperfecta (OI) comprises a heterogeneous group of connective tissue disorders characterized by bone fragility with susceptibility to fractures. Most cases of OI are caused by dominant mutations in *COL1A1* or *COL1A2*, the genes encoding the two type I procollagen alpha chains, proα1 (I) and proα2 (I) [(1)]. Mutations in these genes result in quantitative and/or qualitative defects in type I collagen production by osteoblasts [(2)]. In addition to dominant collagen I mutations, other cases of recessive OI are caused by mutations in proteins that are collagen I modifiers and chaperones, such as the multiple members of the collagen 3-hydroxylation complex [(3-7)].

*Address correspondence to: Thomas L. Clemens, Ph.D., Department of Orthopaedic Surgery, Johns Hopkins University School of Medicine, 601 N. Caroline Street, Baltimore, MD 21287, Tclemen5@jhmi.edu.

OI Type VI is a moderate to severe, recessive form of the disease in which patients typically present with fractures during infancy [8], malformed bones, and frequently have limited mobility by the time they reach adolescence. OI type VI is distinct from other types of OI in that the afflicted subjects display an osteomalacia-like phenotype characterized by thickened osteoid and delayed mineralization. A distinct 'fish-scale' lamellar appearance of the bone has also been noted in bone biopsies [8]. In addition, bisphosphonates are generally less effective in treating type VI than other subtypes of OI [9].

The molecular basis of OI type VI was recently identified as an inactivating mutation in the *SERPINF1* gene, which encodes Pigment Epithelium-Derived Factor (PEDF) [10-13]. *SERPINF1* resides on chromosome 17p13.3 and encodes a 1.5kb transcript that is translated into a 50kDa secreted glycoprotein [14]. Originally isolated from retinal epithelium and characterized for its neurotropic and anti-angiogenic properties [15, 16], PEDF is ubiquitously expressed in both human and mouse [17] and has been implicated in cell cycle control [18], fat metabolism [19], and tumorgenicity [20]. PEDF has been reported to bind the receptor adipose triglyceride lipase (ATGL/desnutrin/iPLA$_{2\zeta}$)[21] in hepatocytes and adipocytes, but the protein also contains binding sites for collagen type I, hyaluroran, the laminin receptor, and heparin, as well as a nuclear localization sequence [14, 22].

In this study we characterized the bone abnormalities in mice lacking Pedf as a first step in determining its function in the skeleton. Our results show that loss of Pedf in mice produce skeletal features which resemble the main defects seen in patients with OI type VI. The availability of this mouse model should enable further studies to more completely understand the function of PEDF in bone and other tissues where it is expressed.

Materials and Methods

Mice

PEDF$^{-/-}$ mice were created as previously described [23]. For all *Pedf*$^{-/-}$ mouse experiments, WT controls were drawn from littermates resulting from *Pedf*$^{+/-}$ X *Pedf*$^{+/-}$ matings. All procedures involving mice were approved by the Institutional Animal Care and Use Committee of The Johns Hopkins University.

Immunohistochemisty

Immunohistochemistry of bone sections was performed using a streptavidin–biotin complex immunoperoxidase technique. Sections were deparaffinized, treated to inhibit endogenous peroxidase and subjected to antigen retrieval as described [23]. All tissues were H&E stained. An experienced pathologist performed all histological evaluations.

MicroCT and histomorphometry

The three-dimensional microarchitecture of the intact right femurs was evaluated using a SkyScan1172 high-resolution micro-CT and its NRecon reconstruction software (Scanco Medical) in accordance with the recommendations of the American Society for Bone and Mineral Research [24]. Quantitative histomorphometry was conducted at distal femoral sites as previously described [25]; serial sections to the stained sections were left unstained for fluorescent microscopy. All parameters comply with the recommendations of the Histomorphometry Nomenclature Committee of the American Society of Bone and Mineral Research [26, 27].

Fourier transform infrared spectroscopy (FTIR))

FTIR was performed on mouse femurs as previously described [28], with the mineral:matrix ratio being calculated as the ratio of the integrated area under the phosphate band (920–

1,180 cm^{-1}) to that of the amide I band (1,585–1,720 cm^{-1}). Means and standard deviations for the three to five images in trabecular and cortical bone were calculated and compared. For the mineral formed in cultures, the culture dishes were air-dried and the mineral scraped from the dish by combination with dry KBr. Pellets formed from these mixtures were analyzed as above.

Mechanical testing

The strength of the femoral mid-shaft was assessed by 3-point bending using a low force mechanical testing system (Bose Electroforce 3100) according to established methods [29-31]. Force-displacement data was used to determine structural properties (ultimate force, ultimate displacement, stiffness, and energy-to-failure).

Osteoblast culture

Primary osteoblasts were isolated from calvarial bones from 1-3 day old neonatal pups via collagenase type I digestion according to standard techniques. Cells were differentiated by supplementing the media with 10 mM β-glycerol phosphate and 50 μg/ml ascorbic acid. Media was changed every 2-3 days. Alkaline phosphatase and alizarin red staining were carried out according to standard techniques. RNA was isolated using Trizol and prepared for quantitative RT-PCR analysis. Primer sequences used for to assess the expression of Pedf, Ank, Npp1, AnxA2, AnxA5, AnxA6, Dmp1, Phex, and Bsp are available upon request.

Statistical analysis

All experiments were repeated at least three times unless otherwise stated and results are expressed as mean ± SEM. For comparisons between two groups of data, the Student's *t*-test was used. $p<0.05$ was considered statistically significant.

Results

Immunohistochemical analysis performed on decalcified bone sections showed positive Pedf immunoreactivity in the osteoblasts lining trabecular surfaces, as well as embedded osteocytes (Fig. 1A). Positive staining was also observed in some osteocytes in cortical bone (not shown). Additionally, Pedf positive immunoreactivity was evident in perivascular cells and the prehypertrophic chondrocytes of the growth plate (data not shown). As shown in Figure 1B, increased CD-31 immunoreactivity was detected in vascular structures from the *Pedf*$^{-/-}$ bones consistent with previous studies demonstrating antiangiogenic properties of Pedf [16].

MicroCT analysis at 12 weeks of age showed that *Pedf*$^{-/-}$ mice had significantly reduced trabecular bone volume fraction in association with reduced trabecular numbers relative to wild-type littermates (Fig. 1C and D). Bone histomorphometry performed at 6 weeks of age revealed no significant differences in the numbers of osteoblasts or osteoclasts in the mutant mice when compared to wild-type controls (Fig. 1E-F). Likewise, bone formation rate was similar in mutant and wild-type mice (Fig. 1G). However, *Pedf*$^{-/-}$ mice exhibited significant increases in osteoid thickness (Fig. 1H) and osteoid maturation time (Fig 1I), suggestive of a defect in the mineralization process. Analysis of bone mineral properties using FTIR demonstrated that like other models of OI [28] the mineral:matrix ratio was significantly increased in *Pedf*$^{-/-}$ mice (Fig 1J). The loss of Pedf function did not affect parameters of cortical bone structure (data not shown) but assessment of cortical bone strength in three-point bending experiments suggested that the bones of *Pedf*$^{-/-}$ mice were more brittle that those of wild-type littermates mice at 12 weeks of age. Ultimate displacement and energy to

failure were significantly reduced in bones from mutant mice (Fig. 1K and M), possibly as a result of the increased mineral:matrix ratio in this bone envelope.

To more directly analyze the role of Pedf on osteoblast function, we examined the effect of Pedf loss of function on osteoblast differentiation *in vitro*. In wild-type osteoblasts, Pedf mRNA expression and protein levels were low or undetectable immediately after plating but steadily increased during osteoblast differentiation with maximal levels evident at day 14 (Fig 2A and B). The increased expression of Pedf at later times during differentiation suggests that the protein normally functions during matrix mineralization. Osteoblasts lacking Pedf appeared to differentiate relatively normally and had similar levels of alkaline phosphatase activity (Fig. 2C). However, matrix mineralization determined by alizarin red staining was increased when compared to cultures of wild-type osteoblasts (Fig 2C) and FTIR measurements performed on mineralized nodules harvested at 14 days showed an increased mineral:matrix ratio of *Pedf*$^{-/-}$ cultures relative to that of wild-type cultures (Fig 2D). The expression of several genes known to be involved in mineralization including annexins and Ank were unaffected in *Pedf*$^{-/-}$osteoblasts whereas RT-PCR analysis revealed the levels of ectonucleotide pyrophosphatase phosphodiesterase 1 (NPP1), Dmp1, Phex and Bsp were reduced relative to wild-type controls (Fig 2E and F).

Discussion

In this study, we characterized a mouse lacking Pedf, the protein product of a gene recently identified to be defective in patients with osteogenesis imperfecta type VI [10-13]. The bone abnormalities in this mouse model closely resemble those seen in patients with OI type VI. The principal defect in bone from *Pedf*$^{-/-}$ mice was the excessive accumulation of unmineralized bone matrix, a phenotype also seen in patients with OI type VI. Moreover, FTIR analysis performed in histological sections from mouse femur and in primary mineralizing osteoblasts suggests that this matrix with an increased mineral to matrix ratio is abnormal, as in other types of OI [28]. Since preliminary analyses indicate the mineral composition is comparable to that in controls (data not shown), it appears that the matrix formed by mutant osteoblasts is unable to support normal mineralization. These features presumably account for the brittle nature of the bones that are more susceptible to fracture. However, precisely how loss of Pedf function causes the abnormal mineral-matrix composition in the mouse or in patients with OI Type VI is still unclear. The reduced expression of several genes involved in bone mineralization in osteoblasts lacking Pedf is consistent with a role for the protein in matrix mineralization. In particular, mouse models with altered expression of Npp1,Dmp1, Phex, or Bsp exhibit defects in bone mineralization [32-35]. It is also possible that the ability of Pedf to control the degree and timing of vascular invasion in developing bone impacts osteoblast development and thereby contributes to the proper accumulation of bone matrix and deposition of mineral. Further studies to explore these potential functions are currently underway and will be facilitated by the mouse models described here.

Another important question relates to the mode of action of Pedf, and in particular whether Pedf is functioning in a cell (osteoblast) autonomous or cell non-autonomous fashion. As described above, Pedf is relatively widely expressed, is secreted into the circulation and could certainly impact bone development through paracrine or hormonal mechanisms. As described above, a number of Pedf receptors have been proposed including ATGL/desnutrin/iPLA$_{2\zeta}$)[21] which are expressed in osteoblasts (data not shown). Alternatively, other studies suggest the possibility that Pedf might function in an intracrine mode through its ability to interact with transcription factors [36, 37]. These potential mechanisms will need to be elucidated using additional models in order to define precisely how Pedf functions in the production of bone matrix to ensure proper development and mineralization of bone.

In summary, the studies presented here confirm Pedf as a critical factor that controls the proper development of bone and ensures its structural integrity by controlling the deposition and mineralization of matrix. Moreover, the mouse model lacking Pedf will continue to provide a very powerful means to elucidate the mechanism through which PEDF impacts bone mineralization and integrity, and causes OI type VI. We predict that the discoveries from such experiments will inform research into more effective treatments for multiple skeletal disorders with mineralization defects.

Acknowledgments

This work was supported by NIH grants AR049410 to TLC and AR043125 to AB. Dr. Riddle is the recipient of a Career Development Award from the Veteran's Administration. Dr. Clemens is a recipient of a Merit Review grant and a research career scientist award from the Veteran's Administration. The authors thank Vandana Singhal for technical assistance and Dr. Douglas DiGirolamo for advice in preparing the manuscript.

References

1. Marini JC, Forlino A, Cabral WA, Barnes AM, San Antonio JD, Milgrom S, Hyland JC, Korkko J, Prockop DJ, De Paepe A, Coucke P, Symoens S, Glorieux FH, Roughley PJ, Lund AM, Kuurila-Svahn K, Hartikka H, Cohn DH, Krakow D, Mottes M, Schwarze U, Chen D, Yang K, Kuslich C, Troendle J, Dalgleish R, Byers PH. Consortium for osteogenesis imperfecta mutations in the helical domain of type I collagen: regions rich in lethal mutations align with collagen binding sites for integrins and proteoglycans. Hum Mutat. 2007; 28:209–221. [PubMed: 17078022]
2. Prockop DJ, Kivirikko KI. Collagens: molecular biology, diseases, and potentials for therapy. Annu Rev Biochem. 1995; 64:403–434. [PubMed: 7574488]
3. Forlino A, Cabral WA, Barnes AM, Marini JC. New perspectives on osteogenesis imperfecta. Nat Rev Endocrinol. 2011; 7:540–557. [PubMed: 21670757]
4. Morello R, Bertin TK, Chen Y, Hicks J, Tonachini L, Monticone M, Castagnola P, Rauch F, Glorieux FH, Vranka J, Bachinger HP, Pace JM, Schwarze U, Byers PH, Weis M, Fernandes RJ, Eyre DR, Yao Z, Boyce BF, Lee B. CRTAP is required for prolyl 3- hydroxylation and mutations cause recessive osteogenesis imperfecta. Cell. 2006; 127:291–304. [PubMed: 17055431]
5. Barnes AM, Chang W, Morello R, Cabral WA, Weis M, Eyre DR, Leikin S, Makareeva E, Kuznetsova N, Uveges TE, Ashok A, Flor AW, Mulvihill JJ, Wilson PL, Sundaram UT, Lee B, Marini JC. Deficiency of cartilage-associated protein in recessive lethal osteogenesis imperfecta. N Engl J Med. 2006; 355:2757–2764. [PubMed: 17192541]
6. Cabral WA, Chang W, Barnes AM, Weis M, Scott MA, Leikin S, Makareeva E, Kuznetsova NV, Rosenbaum KN, Tifft CJ, Bulas DI, Kozma C, Smith PA, Eyre DR, Marini JC. Prolyl 3-hydroxylase 1 deficiency causes a recessive metabolic bone disorder resembling lethal/severe osteogenesis imperfecta. Nat Genet. 2007; 39:359–365. [PubMed: 17277775]
7. Barnes AM, Carter EM, Cabral WA, Weis M, Chang W, Makareeva E, Leikin S, Rotimi CN, Eyre DR, Raggio CL, Marini JC. Lack of cyclophilin B in osteogenesis imperfecta with normal collagen folding. N Engl J Med. 2010; 362:521–528. [PubMed: 20089953]
8. Glorieux FH, Ward LM, Rauch F, Lalic L, Roughley PJ, Travers R. Osteogenesis imperfecta type VI: a form of brittle bone disease with a mineralization defect. J Bone Miner Res. 2002; 17:30–38. [PubMed: 11771667]
9. Land C, Rauch F, Travers R, Glorieux FH. Osteogenesis imperfecta type VI in childhood and adolescence: effects of cyclical intravenous pamidronate treatment. Bone. 2007; 40:638–644. [PubMed: 17127117]
10. Becker J, Semler O, Gilissen C, Li Y, Bolz HJ, Giunta C, Bergmann C, Rohrbach M, Koerber F, Zimmermann K, de Vries P, Wirth B, Schoenau E, Wollnik B, Veltman JA, Hoischen A, Netzer C. Exome sequencing identifies truncating mutations in human SERPINF1 in autosomal-recessive osteogenesis imperfecta. Am J Hum Genet. 2011; 88:362–371. [PubMed: 21353196]
11. Homan EP, Rauch F, Grafe I, Lietman C, Doll JA, Dawson B, Bertin T, Napierala D, Morello R, Gibbs R, White L, Miki R, Cohn DH, Crawford S, Travers R, Glorieux FH, Lee B. Mutations in

SERPINF1 cause osteogenesis imperfecta type VI. J Bone Miner Res. 2011; 26:2798–2803. [PubMed: 21826736]

12. Tucker T, Nelson T, Sirrs S, Roughley P, Glorieux FH, Moffatt P, Schlade-Bartusiak K, Brown L, Rauch F. A co-occurrence of osteogenesis imperfecta type VI and cystinosis. Am J Med Genet A. 2012; 158A:1422–1426. [PubMed: 22528245]
13. Venturi G, Gandini A, Monti E, Dalle Carbonare L, Corradi M, Vincenzi M, Valenti MT, Valli M, Pelilli E, Boner A, Mottes M, Antoniazzi F. Lack of expression of SERPINF1, the gene coding for pigment epithelium-derived factor, causes progressively deforming osteogenesis imperfecta with normal type I collagen. J Bone Miner Res. 2012; 27:723–728. [PubMed: 22113968]
14. Tombran-Tink J, Aparicio S, Xu X, Tink AR, Lara N, Sawant S, Barnstable CJ, Zhang SS. PEDF and the serpins: phylogeny, sequence conservation, and functional domains. J Struct Biol. 2005; 151:130–150. [PubMed: 16040252]
15. Tombran-Tink J, Chader GG, Johnson LV. PEDF: a pigment epithelium-derived factor with potent neuronal differentiative activity. Exp Eye Res. 1991; 53:411–414. [PubMed: 1936177]
16. Dawson DW. Pigment Epithelium-Derived Factor: A Potent Inhibitor of Angiogenesis. Science. 1999; 285:245–248. [PubMed: 10398599]
17. Ek ET, Dass CR, Choong PF. PEDF: a potential molecular therapeutic target with multiple anti-cancer activities. Trends Mol Med. 2006; 12:497–502. [PubMed: 16962374]
18. Filleur S, Nelius T, de Riese W, Kennedy RC. Characterization of PEDF: a multi-functional serpin family protein. J Cell Biochem. 2009; 106:769–775. [PubMed: 19180572]
19. Chung C, Doll JA, Gattu AK, Shugrue C, Cornwell M, Fitchev P, Crawford SE. Anti-angiogenic pigment epithelium-derived factor regulates hepatocyte triglyceride content through adipose triglyceride lipase (ATGL). J Hepatol. 2008; 48:471–478. [PubMed: 18191271]
20. Ho TC, Chen SL, Shih SC, Chang SJ, Yang SL, Hsieh JW, Cheng HC, Chen LJ, Tsao YP. Pigment epithelium-derived factor (PEDF) promotes tumor cell death by inducing macrophage membrane tumor necrosis factor-related apoptosis-inducing ligand (TRAIL). J Biol Chem. 2011; 286:35943–35954. [PubMed: 21846721]
21. Notari L, Baladron V, Aroca-Aguilar JD, Balko N, Heredia R, Meyer C, Notario PM, Saravanamuthu S, Nueda ML, Sanchez-Sanchez F, Escribano J, Laborda J, Becerra SP. Identification of a lipase-linked cell membrane receptor for pigment epithelium-derived factor. J Biol Chem. 2006; 281:38022–38037. [PubMed: 17032652]
22. Anguissola S, McCormack WJ, Morrin MA, Higgins WJ, Fox DM, Worrall DM. Pigment Epithelium-Derived Factor (PEDF) Interacts with Transportin SR2, and Active Nuclear Import Is Facilitated by a Novel Nuclear Localization Motif. PLoS One. 2011; 6:e26234. [PubMed: 22028839]
23. Doll JA, Stellmach VM, Bouck NP, Bergh AR, Lee C, Abramson LP, Cornwell ML, Pins MR, Borensztajn J, Crawford SE. Pigment epithelium-derived factor regulates the vasculature and mass of the prostate and pancreas. Nat Med. 2003; 9:774–780. [PubMed: 12740569]
24. Bouxsein ML, Boyd SK, Christiansen BA, Guldberg RE, Jepsen KJ, Muller R. Guidelines for assessment of bone microstructure in rodents using micro-computed tomography. J Bone Miner Res. 2010; 25:1468–1486. [PubMed: 20533309]
25. Zhang M, Xuan S, Bouxsein ML, von Stechow D, Akeno N, Faugere MC, Malluche H, Zhao G, Rosen CJ, Efstratiadis A, Clemens TL. Osteoblast-specific knockout of the insulin-like growth factor (IGF) receptor gene reveals an essential role of IGF signaling in bone matrix mineralization. J Biol Chem. 2002; 277:44005–44012. [PubMed: 12215457]
26. Parfitt AM, Drezner MK, Glorieux FH, Kanis JA, Malluche H, Meunier PJ, Ott SM, Recker RR. Bone histomorphometry: standardization of nomenclature, symbols, and units. Report of the ASBMR Histomorphometry Nomenclature Committee. J Bone Miner Res. 1987; 2:595–610. [PubMed: 3455637]
27. Dempster DW, Compston JE, Drezner MK, Glorieux FH, Kanis JA, Malluche H, Meunier PJ, Ott SM, Recker RR, Parfitt AM. Standardized nomenclature, symbols, and units for bone histomorphometry: A 2012 update of the report of the ASBMR Histomorphometry Nomenclature Committee. J Bone Miner Res. 2013; 28:2–17. [PubMed: 23197339]

28. Coleman RM, Aguilera L, Quinones L, Lukashova L, Poirier C, Boskey A. Comparison of bone tissue properties in mouse models with collagenous and non-collagenous genetic mutations using FTIRI. Bone. 2012; 51:920–928. [PubMed: 22910579]

29. Brodt MD, Ellis CB, Silva MJ. Growing C57Bl/6 mice increase whole bone mechanical properties by increasing geometric and material properties. J Bone Miner Res. 1999; 14:2159–2166. [PubMed: 10620076]

30. Jepsen KJ, Pennington DE, Lee YL, Warman M, Nadeau J. Bone brittleness varies with genetic background in A/J and C57BL/6J inbred mice. J Bone Miner Res. 2001; 16:1854–1862. [PubMed: 11585350]

31. Ritchie RO, Koester KJ, Ionova S, Yao W, Lane NE, Ager JW 3rd. Measurement of the toughness of bone: a tutorial with special reference to small animal studies. Bone. 2008; 43:798–812. [PubMed: 18647665]

32. Ling Y, Rios HF, Myers ER, Lu Y, Feng JQ, Boskey AL. DMP1 depletion decreases bone mineralization in vivo: an FTIR imaging analysis. J Bone Miner Res. 2005; 20:2169–2177. [PubMed: 16294270]

33. Yuan B, Takaiwa M, Clemens TL, Feng JQ, Kumar R, Rowe PS, Xie Y, Drezner MK. Aberrant Phex function in osteoblasts and osteocytes alone underlies murine X-linked hypophosphatemia. J Clin Invest. 2008; 118:722–734. [PubMed: 18172553]

34. Mackenzie NC, Huesa C, Rutsch F, MacRae VE. New insights into NPP1 function: lessons from clinical and animal studies. Bone. 2012; 51:961–968. [PubMed: 22842219]

35. Malaval L, Wade-Gueye NM, Boudiffa M, Fei J, Zirngibl R, Chen F, Laroche N, Roux JP, Burt-Pichat B, Duboeuf F, Boivin G, Jurdic P, Lafage-Proust MH, Amedee J, Vico L, Rossant J, Aubin JE. Bone sialoprotein plays a functional role in bone formation and osteoclastogenesis. J Exp Med. 2008; 205:1145–1153. [PubMed: 18458111]

36. Chung C, Doll JA, Stellmach VM, Gonzales J, Surapureddi S, Cornwell M, Reddy JK, Crawford SE. Pigment epithelium-derived factor is an angiogenesis and lipid regulator that activates peroxisome proliferator-activated receptor alpha. Adv Exp Med Biol. 2008; 617:591–597. [PubMed: 18497086]

37. Tombran-Tink J, Barnstable CJ. PEDF: a multifaceted neurotrophic factor. Nat Rev Neurosci. 2003; 4:628–636. [PubMed: 12894238]

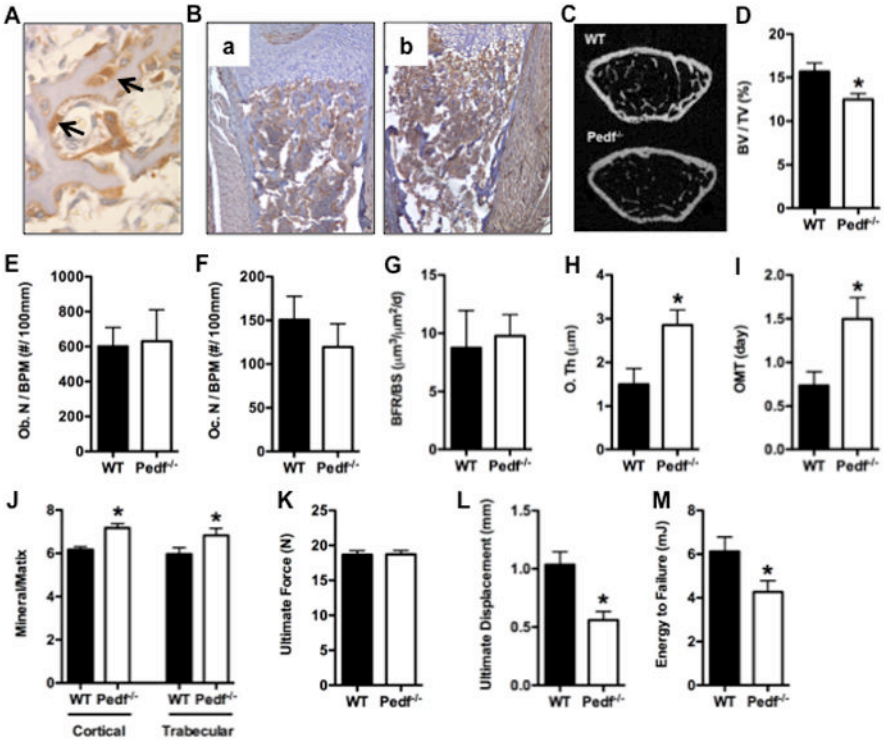

Figure 1. PEDF expression and loss of function in vivo

(A) Immunohistochemical staining of PEDF in osteoblasts (arrows) in trabecular bone from a wild type mouse. (B) CD31 staining in bone from wild type (a) and Pedf$^{-/-}$ mice (b). (C-D) Quantitative micro-CT analysis of the distal femur in wild-type (WT) and Pedf$^{-/-}$ mice at 12-weeks of age (n=4–5mice). (C) Representative images. (D) Bone volume/tissue volume, BV/TV (%). (E-I) Histomorphometric analysis of the distal femoral metaphysis in male wild-type and Pedf$^{-/-}$ mice at 6-weeks of age (n=5–7mice). (E) Osteoblast Number per bone perimeter, Ob. N/BPM (no./100mm) at 6 weeks of age. (F) Osteoclast Number per bone perimeter at 6 weeks of age. (G) Bone formation rate per bone surface, BFR/BS, mm^3/cm^2/yr. (H) Osteoid thickness (uM). (I) Osteoid maturation time (days). (J) FTIR measures of mineral:matrix ratios in cortical and trabecular bone. (K-M) Three-point bending analysis of femurs in wild-type and PEDF$^{-/-}$ mice (n = 5–8 mice). (K) Ultimate force (N). (L) Ultimate displacement (mm). (M) Energy to Failure (mJ). All error bars represent SEM. *$p < 0.05$

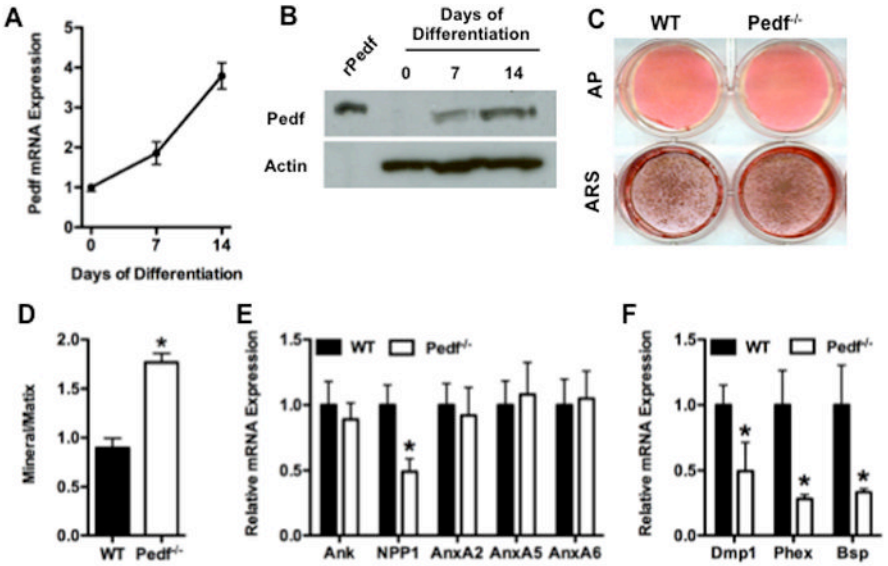

Figure 2. PEDF expression and loss of function in primary cultultured osteoblasts

(A) Relative expression levels of mRNA in samples collected in freshly plated osteoblasts (day 0) and at 7 and 14 days of culture in differentiation medium. (B) Western blot of Pedf protein levels in osteoblasts from wild type mice at the indicated times in culture. Actin used as loading control. (C) Examination of osteoblast differentiation in wild-type and Pedf$^{-/-}$ osteoblasts. Alkaline phosphatase (ALP) and Alizarin Red (ARS) staining after 7 and 14 days of differentiation, respectively. (D) Mineral:matrix ratio of cultured osteoblasts. (E) RT-PCR analysis of Ank, NPP1, Annexins 2, 5 and 6 expression performed at 14 days of differentiation. (F) RT-PCR analysis of Dmp1, Phex and Bsp expression at day 14. All error bars represent SEM. *$p < 0.05$